Transgenic Res (2013) 22:425–434
DOI 10.1007/s11248-012-9654-7

BRIEF COMMUNICATION

Mammary gland development is delayed in mice deficient for aminopeptidase N

Andreas F. Kolb · David Sorrell · Caroline Lassnig · Simon Lillico · Ailsa Carlisle · Claire Neil · Claire Robinson · Mathias Müller · C. Bruce A. Whitelaw

Received: 15 June 2012 / Accepted: 5 September 2012 / Published online: 15 September 2012

Abstract Development of the mammary gland requires the coordinated action of proteolytic enzymes during two phases of remodelling. Firstly, new ducts and side-branches thereof need to be established during pregnancy to generate an extensive ductal tree allowing the secretion and transport of milk. A second wave of remodelling occurs during mammary involution after weaning. We have analysed the role of the cell surface protease aminopeptidase N (Anpep, APN, CD13) during these processes using Anpep deficient and Anpep over-expressing mice. We find that APN deficiency significantly delays mammary gland morphogenesis during gestation. The defect is characterised by a reduction in alveolar buds and duct branching at mid-pregnancy. Conversely over-expression of Anpep leads to accelerated ductal development. This indicates that Anpep plays a critical role in the proteolytic remodelling of mammary tissue during adult mammary development.

Keywords Mammary gland · Protease · Gene locus · Homologous recombination · Development

Abbreviations

APN, Anpep	Aminopeptidase N
BAC	Bacterial artificial chromosome
ES cells	Embryonic stem cells
HRP	Horse radish peroxidase
MMP	Matrix metallo-proteinase
PCR	Polymerase chain reaction

Introduction

The mammary gland undergoes extensive tissue remodelling during each lactation cycle. During pregnancy, the epithelial compartment of the gland is vastly expanded (Benaud et al. 1998). At the end of lactation the epithelial cells undergo apoptosis, and adipocyte differentiation is induced (Lilla et al. 2002). Ductal and alveolar growth during puberty and pregnancy, and the involution process require the

A. F. Kolb (✉)
Metabolic Health Division, Rowett Institute of Nutrition & Health, University of Aberdeen, Aberdeen AB21 9SB, Scotland, UK
e-mail: A.kolb@abdn.ac.uk

A. F. Kolb · D. Sorrell · C. Robinson
Molecular Recognition Group, Hannah Research Institute, Ayr, UK

Present Address:
D. Sorrell
Horizon Discovery Ltd., 7100 Cambridge Research Park, Cambridge CB25 9TL, UK

C. Lassnig · M. Müller
Institute of Animal Genetics & Biomodels, University of Veterinary Medicine Vienna, Vienna, Austria

S. Lillico · A. Carlisle · C. Neil · C. B. A. Whitelaw
Department of Developmental Biology, Roslin Institute, Roslin, UK

action of proteolytic enzymes (including matrix metallo-proteinases, plasminogen and membrane-peptidases) and the corresponding genes are activated during these periods (Benaud et al. 1998; Alexander et al. 2001). Matrix metallo-proteinases (MMPs) are expressed in several cell types of the mammary gland including stromal fibroblasts (e.g. MMP3, MMP2), epithelial cells (e.g. MMP7 or MMP9), adipocytes (e.g. MMP2) and lymphoid cells (e.g. MMP9) (Crawford and Matrisian 1996; Lund et al. 1996; Wiseman et al. 2003). A number of knock-out mice which are deficient for individual MMPs (e.g. MMP2, MMP3) or plasminogen display alterations to mammary gland structure and impairment of lactation (Wiseman et al. 2003; Lund et al. 1999).

Mammary gland involution proceeds in two distinct phases: a first, potentially p53-dependent, partly reversible phase characterised by epithelial apoptosis and a second, p53-independent, irreversible phase characterised by extensive tissue remodelling and adipocyte proliferation (Lund et al. 1996; Jerry et al. 1998; Li et al. 1996). Proteolytic enzymes are induced during the second phase of involution suggesting that their expression is a consequence of epithelial cell apoptosis rather than a pre-requisite. Nevertheless, matrix-interactions provide survival signals to the mammary epithelium, such that removal of these signals can enhance apoptosis (Farrelly et al. 1999; Gilmore et al. 2000). Proteolytic breakdown products of matrix components like fibronectin can induce apoptosis in some mammary cell lines (Schedin et al. 2000). Proteinase activity may therefore accelerate the apoptosis of the epithelium, whilst stimulating differentiation of adipocytes via matrix remodelling (Alexander et al. 2001).

Aminopeptidase N (Anpep, APN) is a cell surface protease which has been implicated in a variety of roles in mammals. It is expressed highly in a variety of tissues including gut, mononuclear blood cells, lung, brain and others. Its expression is elevated during inflammatory processes and during tumorigenesis. It also acts as a receptor for type II coronaviruses (Yeager et al. 1992; Delmas et al. 1994) and (in case of the human Anpep) human cytomegalovirus. Experiments carried out in vitro and in Anpep deficient mice (allele description: Anpep<tm1Sid>) have demonstrated a critical role for Anpep in neo-vascularisation (Guzman-Rojas et al. 2012; Rangel et al. 2007b; Bhagwat et al. 2001). In contrast, Anpep has been shown to be dispensable for normal haematopoiesis and myeloid cell function in mice (allele description: Anpep<tm1.1Lsha>) (Winnicka et al. 2010). In the mammary gland Anpep is expressed with a similar pattern as other proteolytic enzymes in that its expression is high during pregnancy and involution and low during lactation (Sorrell et al. 2005). We therefore speculated that Anpep may also play a role during mammary gland development and have addressed this question using mice deficient in Anpep and transgenic mice over-expressing Anpep (Lassnig et al. 2005). We find that Anpep deficiency significantly impairs the formation of side branches of mammary ducts during pregnancy. Over-expression of Anpep, in contrast, enhances ductal side-branching during pregnancy. These data demonstrate that Anpep plays an important role in the proteolytic remodelling during the mammary development cycle.

Materials and methods

Gene targeting

The murine Anpep gene was isolated from a BAC library (Research Genetics). The gene was identified in the BAC pools using the primer pair mAPN1/mAPN2R (Table 1). The targeting construct was generated using an upstream region of homology of 1364 bp corresponding to the region of −450 to +914 bp (with regards to the transcriptional start site) and a downstream region of homology of 6,215 bp corresponding to the region from +4,375 to +10,590 bp. The upstream region of homology was isolated as a XhoI/HindIII fragment and the downstream region was isolated as a SphI/XhoI fragment. A PGKneo selection marker gene was inserted between the two regions of homology. The targeting event removes exons 2–9 (which encode the catalytic domain) from the Anpep gene. The first exon remains intact; however potential transcripts fusing exon 1 to exon 10 will lead to a frameshift and the generation of a stop codon in the second codon of exon 10, thereby leading to a truncated protein containing the first 207 amino acids of the Anpep protein (whereas the full length protein consists of 967 amino acid).

The targeting construct was tested in HM1 mouse ES cells and analysed by PCR and Southern blot analysis. For the genotyping PCR in ES cells the

Table 1 Primer combinations used for PCR genotyping and RT-PCR

Name	Sequence	Annealing temp. (°C)	Amplicon length (bp)
mAPN14	5′ GCT TCA TTC TGC TCT GCC TGC CTT ACC TC 3′		
mAPN15R	5′ CCA GGC TCA CCT TTG GGA AGC ATA TTA GA 3′	60	1,687
mAPN14	5′ GCT TCA TTC TGC TCT GCC TGC CTT ACC TC 3′		
PGK5	5′ AAG CGC ATG CTC CAG ACT GCC TTG GGA AA 3′	61	1,507
mAPN10	5′ AAG CTC AAC TAC ACC CTC AAA G 3′		
mAPN15R	5′ CCA GGC TCA CCT TTG GGA AGC ATA TTA GA 3′	55	801
mAPN10	5′ AAG CTC AAC TAC ACC CTC AAA G 3′		
PGK5	5′ AAG CGC ATG CTC CAG ACT GCC TTG GGA AA 3′	55	623
mAPN1	5′ CTT GGG CAT CCT GTT GGG T 3′		
mAPN2R	5′ GAT TTC CGA GCA TCA GCA GC 3′	62	621
β-actin1	5′ GTC GAC AAC GGS TCC GSC ATG TG 3′		
β-actin2	5′ CTG TCR GCR ATG CCW GGG TAC AT 3′	60	908

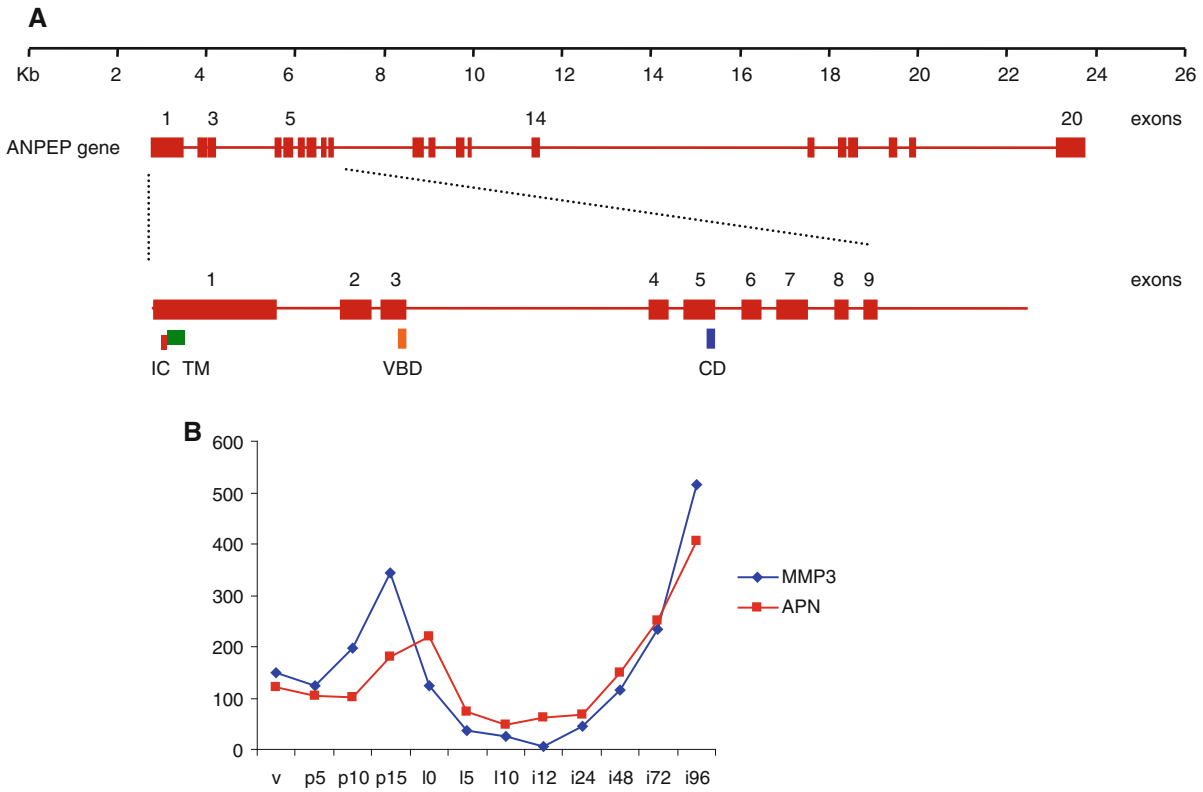

Fig. 1 **a** Important domains of the Anpep protein: *IC* intracellular domain, *TM* trans-membrane domain, *VBD* region homologous to the binding domain for HCoV229E in the human Anpep protein, *CD* catalytic domain. Exons of the Anpep gene are indicated as *red boxes*. The *numbers above* the *boxes* indicate the number of the exon. **b** Expression profile of the genes encoding aminopeptidase N (APN) and stromelysin 1 (MMP3) during mammary gland development as measured by micro-array (in arbitrary units): [v] virgin (age in weeks), [p] pregnant [l] lactating (in days) [i] involuting (in hours) (Clarkson et al. 2004). (Colour figure online)

primer combination mAPN14/mAPN15R/PGK5 was used. The primer pair mAPN14/mAPN15R yields a 1,687 bp fragment from the unmodified Anpep gene. The primer pair mAPN14/PGK5 gives rise to a 1,507 bp fragment from a targeted Anpep allele. The targeting frequency was 2.9 % (7 targeted ES cell clones in 240 clones analysed). Southern blot analysis was carried out as described (Kolb and Siddell 1997).

The knock-out mice were generated by Genoway (Lyon, France) using their standard protocols. The targeting construct was transfected into SV129 derived ES cells and positive cell clones (as identified by PCR analysis) were transferred into C57BL/6J hosts. The new mutant Anpep allele will be referred to as Anpep<tm1Afk>. Chimeric mice were bred onto a C57BL/6J background to derive animals which transmit the mutant allele through the germline. These founder mice were then transferred to the mouse facility at the Roslin Institute and maintained in accordance with UK Home Office regulations. The mice were maintained on a C57BL/6J background. The phenotype documented in this paper was observed after 3, 7 and 10 generations of breeding onto the C57BL/6J background. The Anpep over-expressing mice were described before (Lassnig et al. 2005).

RT-PCR

RNA was isolated from mouse tissues using RNAwiz (Ambion) according to the manufacturer's recommendation. 1 μg of total RNA was reverse transcribed using MLV-RT (Promega) and an oligo-dT primer. 1/50 of the cDNA synthesis solution was used for PCR using the primer pairs β-actin1/β-actin2 and mAPN1/mAPN2R (Table 1).

Protein analysis

Whole cell extracts from mouse tissues were prepared in RIPA buffer (20 mM Tris–HCl (pH 7.5), 150 mM NaCl, 1 mM Na_2EDTA, 1 mM EGTA, 1 % NP-40, 1 % sodium deoxycholate, 2.5 mM sodium pyrophosphate, 1 mM β-glycerophosphate, 1 mM Na_3VO_4, 1 μg/ml leupeptin). 1 mg of extracts was immunoprecipitated with 5 μl of the Anpep rat monoclonal antibody R3-242 (Research Diagnostics). The precipitated protein was then separated on a 6.5 % SDS-polyacrylamide gel and blotted to nitrocellulose. The Anpep protein was detected using a mouse Anpep specific M17 goat-serum (sc-6996, Santa Cruz Biotechnology). The ubiquitously expressed protein Stat1 was used as a control. Stat1 protein was immunoprecipitated from the 1 mg of tissue extracts using 5 μl of the rabbit anti-αp91-Stat1 serum M23 (sc-591, Santa Cruz Biotechnology) and detected using the same serum after western blotting. Antibodies in the western blot were used at a dilution of 1:1,000.

Fig. 2 **a** Genomic structure of the unmodified and the targeted APN gene. APN exons are indicated as *red boxes*. The positions of the primer combinations used for the PCR genotyping are indicated as *arrows*; the sizes of the expected PCR products are shown in *square brackets*. The probes used for Southern blot analysis are shown as *green boxes*. The expected fragments hybridising with these probes are shown as *green lines*. **b** PCR analysis of genomic DNA derived from one of the targeted cell clones and the parental HM1 ES cells. 100 ng of genomic DNA were amplified using the primer combination mAPN14, mAPN15R and PGK5. The 1,687 bp product is indicative of the unmodified APN gene, whereas the 1,509 bp product indicates a successful targeting event at the APN gene. The PCR reactions were separated on a 2 % agarose gel and the products visualised by staining with ethidium bromide. Phage λ DNA digested with HindIII and EcoRI was used as marker. **c** PCR analysis of genomic DNA derived from transgenic mice. 100 ng of genomic DNA were amplified using the primer combination mAPN10, mAPN15R and PGK5. The 801 bp product is indicative of the unmodified APN gene, whereas the 623 bp product indicates a successful targeting event at the APN gene. **d** Southern blot analysis of the 5′ end of the APN gene. BglII digested genomic DNA was analysed using the probe indicated in **a**. The 5.1 kb band is indicative of a targeted APN gene, the 4 kb band is indicative of the unmodified APN gene. **e** Southern blot of the 3′ end of the APN gene. SalI/BstEII digested DNA was analysed using the probe indicated in **a**. The 12.4 kb band is indicative of a targeted APN gene, the 13.7 kb band is indicative of the unmodified APN gene. (Color figure online)

Whole mounts

Whole mounts of mammary glands were prepared as described with modifications (Tonner et al. 2002). Briefly, individual mammary glands were placed on poly-lysine coated microscope slides, carefully spread with forceps and allowed to air dry for 10 min. They were then fixed in Carnoy's reagent (60 % ethanol, 30 % chloroform, 10 % glacial acetic acid) over night and washed in 70 % ethanol for 15 min followed by a rinse in distilled water. The slides were then stained overnight in a solution of 0.1 % carmine, 0.25 % aluminium potassium sulphate. After overnight staining, the gland was washed for 15 min in 70, 95 and

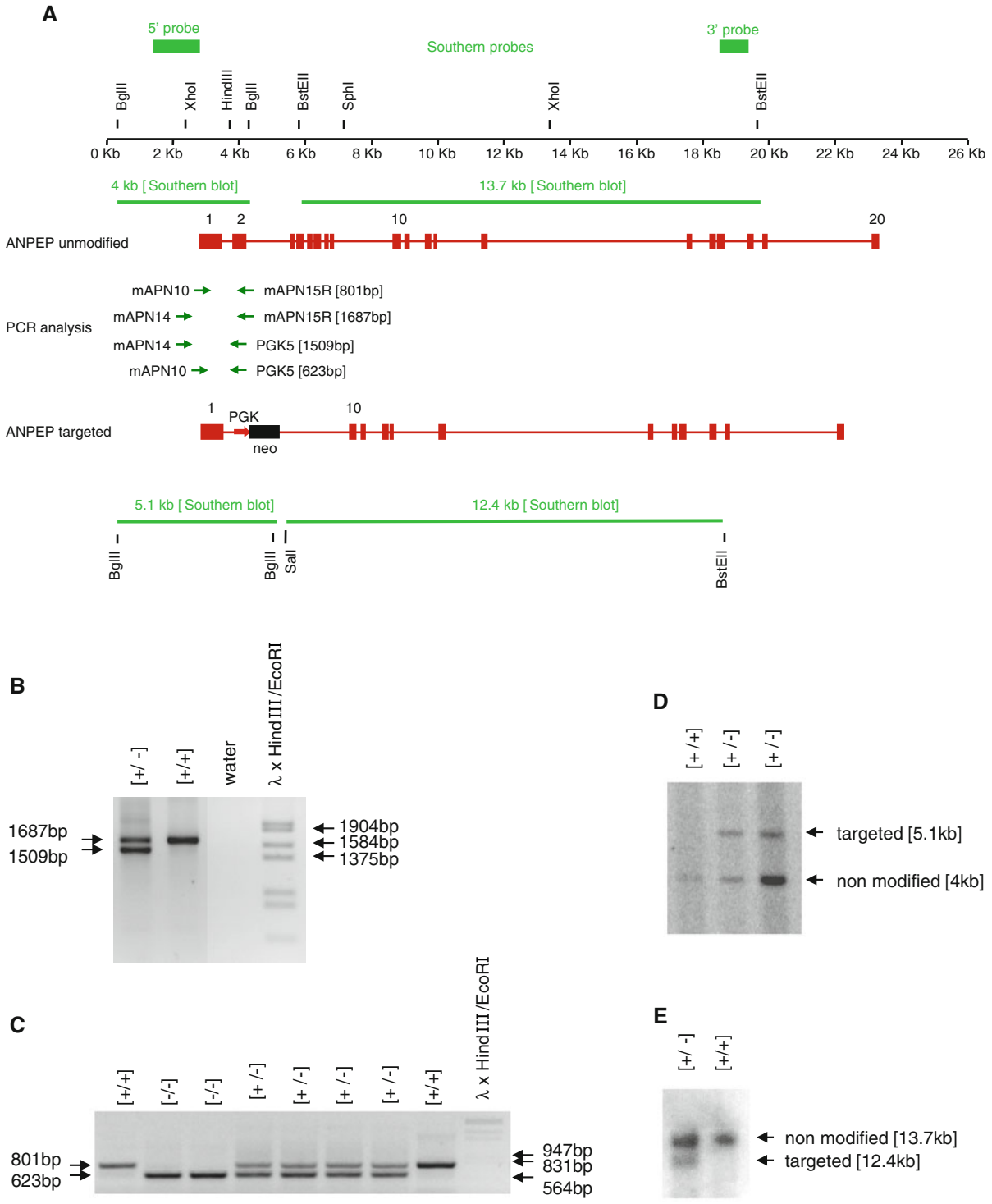

100 % ethanol for 15 min each before immersion in Histoclear for 5 min and finally mounting in DPX (VWR International).

Duct area in the fat pads was determined using Adobe Photoshop. The number of alveolar buds, junctions and distance between side branches were

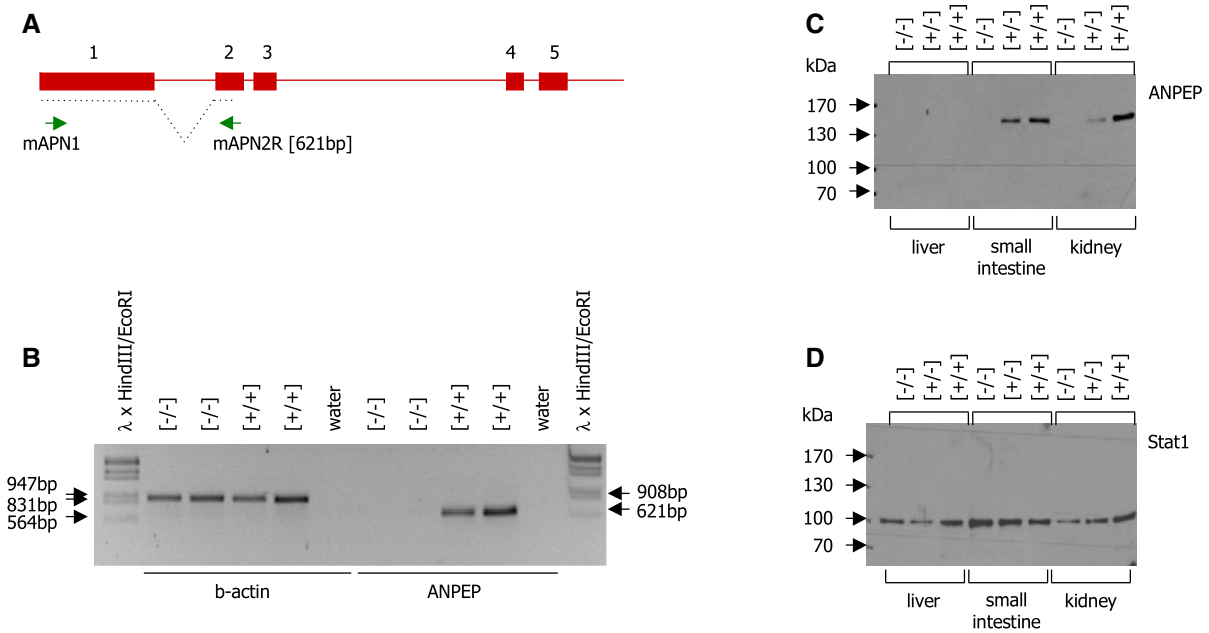

Fig. 3 Analysis of APN expression. **a** Schematic representation of the first 5 exons of the mouse APN gene. The positions of the oligonucleotides (mAPN1/mAPN2R) used for the RT-PCR analysis are indicated; the size of the expected PCR product is shown in *square brackets*. **b** RT-PCR analysis of RNA isolated from small intestine tissue of two APN deficient and two control mice using a primer pair specific for the mouse β-actin gene (β-actin1/2) and a primer pair specific for APN (mAPN1/2R). Aliquots of the PCR reaction were separated on a 2 % agarose gel alongside a DNA size marker (phage λ digested with HindIII/EcoRI). The expected β-actin specific PCR product could be detected in all four RNA samples, whereas the APN specific product could only be detected in the control samples. **c** Western blot analysis of APN protein expression in protein samples isolated from liver, small intestine and kidney of APN deficient mice [−/−], heterozygous mice [−/+] and control mice [+/+]. Aliquots of the protein samples were immuno-precipitated using a rat-anti mouse APN antiserum and separated on a 10 % protein gel. The proteins were blotted to nitrocellulose and detected using an APN specific antiserum and an HRP linked secondary antiserum. **d** As a loading control the protein samples were immuno-precipitated with a rabbit antiserum directed against mouse Stat1 protein, probed with the same antiserum and developed using a HRP-linked secondary antiserum

determined and recorded using Image J. The data were analysed statistically using one way ANOVA.

Results

In order to study the role of aminopeptidase N during mammary gland development, we generated Anpep deficient mice. The targeting event removes exons 2 through 9 which include the catalytic centre of Anpep and the region corresponding to the binding domain for the human coronavirus 229E (Fig. 1). Targeting of the Anpep gene was detected by using PCR using primer combinations which yield characteristic PCR products for the endogenous and targeted allele (Fig. 2b, c). The PCR data were confirmed by Southern blotting as shown in Fig. 2d, e. Expression of Anpep was assessed in Anpep knock-out and control mice using RT-PCR on RNA isolated from small intestine tissue of two Anpep knock-out mice and two control mice. As expected the PCR product indicative of Anpep expression was lost in the Anpep knock-out mice, whereas a PCR product indicative of β-actin was detectable in all mice (Fig. 3b). This was confirmed by western blot analysis of Anpep protein in total cellular protein extracts derived from liver, small intestine and kidney (Fig. 3c). Significant amounts of Anpep are detectable in kidney and small intestine of wild-type mice. Heterozygous mice show a reduced amount of Anpep expression, whereas no Anpep expression is detectable in Anpep knock-out mice. The absence of an Anpep specific signal in liver tissue is presumably due to the fact that the glycosylation pattern of Anpep in that tissue is not detected by the antibody used. Anpep-specific mRNA

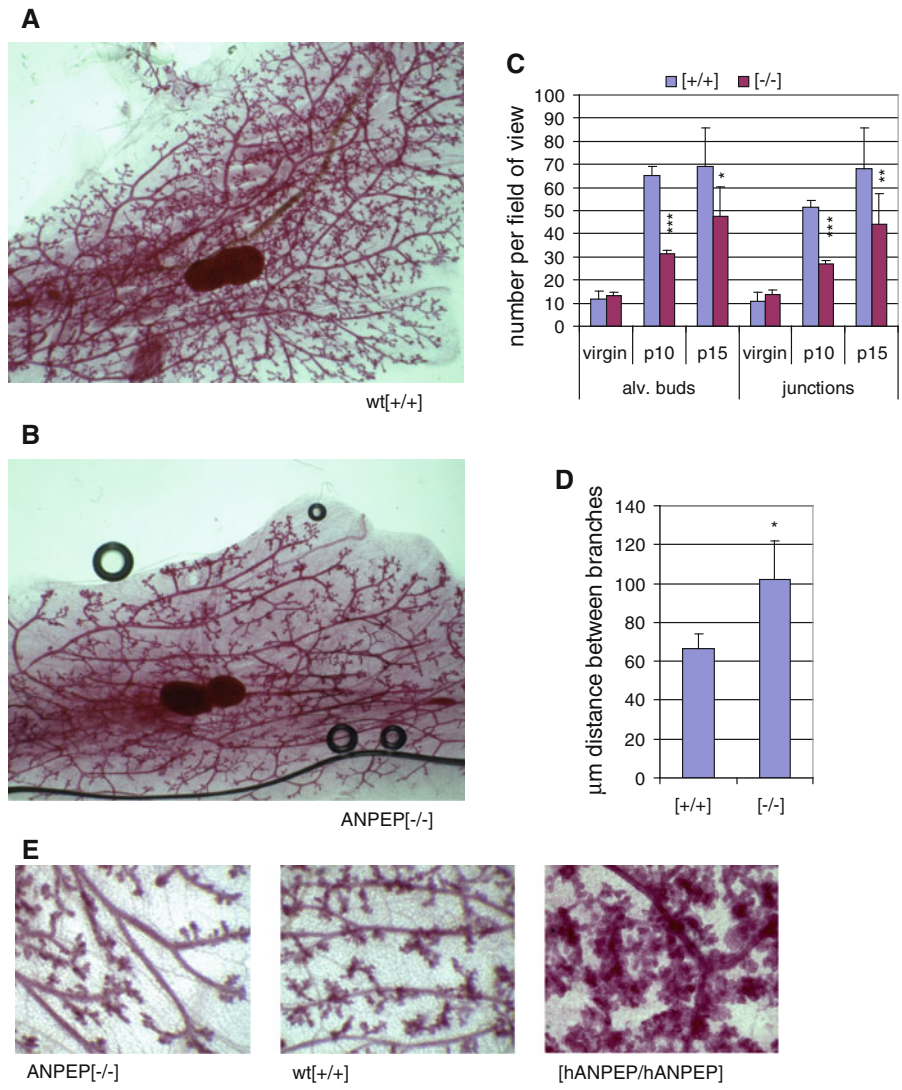

Fig. 4 Whole mount analysis of mammary tissue. **a** Mammary gland whole mount of a typical control mouse at day 10 of gestation at a 10× magnification. **b** Mammary gland whole mount of a typical APN deficient mouse at day 10 of gestation. **c** Number of alveolar buds and junctions of side-branches in the mammary glands of virgin mice (virgin), mice at day 10 of gestation (p10) and day 15 of gestation (p15). Gland numbers analysed: virgin: n = 4 (from 2 mice), p10: n = 6 (from 3 mice), p15: n = 10 (from 5 mice) in each group. **d** Average distance between side-branches in control [+/+] and APN deficient mice [−/−] at day 10 of gestation. Six different glands (from 3 mice) were analysed for each group. Data were analysed by one way ANOVA; $*p < 0.5$, $**p < 0.01$, $***p < 0.001$. *Error bars* indicate standard deviations. **e** Mammary gland whole mounts of an APN deficient [−/−], a wild-type [+/+] and a homozygous hANPEP [hANPEP/hANPEP] mouse at day 10 of lactation

in liver tissue can be detected at expression levels of 10 % of those found in the small intestine (data not shown). Similar amounts of the control protein Stat1 are detectable in all protein samples (Fig. 3d). We did not observe any overt abnormalities in the Anpep deficient mice during their normal life cycle. The mice produced offspring at the expected Mendelian ratio and did not show any deficiencies in terms of fertility. This is comparable to findings in the two previously generated Anpep deficient mouse strains (Rangel et al. 2007a; Winnicka et al. 2010).

In order to assess the effect of Anpep deficiency on mammary gland development we assessed whole mounts of mammary tissue at various stages of the mammary developmental cycle (data not shown). Consistent with results in other gene deficient mice we find that the best time point to observe differences in mammary development is between day 10 and day 15 of gestation. At this stage a clear difference in side branching of mammary ducts is detectable between Anpep deficient and control mice (Fig. 4a, b). Anpep deficiency leads to a lower number of alveolar buds ($p < 0.001$ for day 10 of gestation and $p < 0.05$ for day 15 of gestation) and side-branch junctions ($p < 0.001$ for day 10 and $p < 0.01$ for day 15 of gestation) (Fig. 4c). Whole mounts from Anpep deficient mice also show an increased distance between side branches ($p < 0.05$) (Fig. 4d). Despite these deficiencies Anpep deficient mice appear to lactate normally as the weight gain

of their offspring is not significantly different to that of control animals. The phenotype documented in this paper was observed after 3, 7 and 10 generations of breeding onto the C57BL/6J background, suggesting that the effect is not impacted by genes which vary between the SV129 and the C57BL/6J mouse strain.

Mice which over-express the human Anpep gene under the control of the porcine Anpep promoter (replicating the expression pattern of the mouse Anpep gene) showed a higher number of side branches at day 10 of gestation thereby producing the reverse phenotype of the Anpep deficient mice (Fig. 4e). Duct area is increased significantly under these conditions. However, this phenotype does not occur with full penetrance due to the differences in transgene expression between individual mice.

Discussion

Proteolytic enzymes play a major role in remodelling the mammary gland during adult development. Two waves of abundant expression of proteases can therefore be detected during pregnancy and involution (Sorrell et al. 2005). There is a high degree of redundancy among the multitude of proteolytic enzymes and no single deficiency is able to completely abrogate mammary gland development. Human Anpep has been detected in intra- and interlobular fibroblasts and on the apical surface of some luminal epithelial cells in the human breast (Atherton et al. 1992). It is also expressed throughout most developmental phases (Atherton et al. 1994a) and can be found on fibroblast explants from human breast (Atherton et al. 1994b). To our knowledge murine Anpep has not been detected successfully in mammary tissue by immuno-histochemistry. This may be due to the fact that most antibodies against Anpep recognise highly variable glycosylation patterns which vary between different tissues. We were able to detect murine Anpep in intestinal tissue, but an identical protocol did not generate Anpep specific signals in the mammary gland.

The data shown in here indicate that Anpep makes a significant contribution to the morphogenesis of the epithelial mammary ducts. The defect detected in Anpep deficient animals is similar to that seen in MMP3 deficient mice, in that the invasion of the terminal endbuds through the stroma is not impaired, but the formation of secondary branches is significantly affected (Wiseman et al. 2003). Furthermore the over-expression of Anpep in the mammary gland leads to an increase in side-branching and a precocious development of the mammary ductal tree; again a phenotype which is similar to the one observed in mice over-expressing MMP3 in the mammary gland (Sternlicht et al. 1999; Witty et al. 1995). This raises the question as to whether Anpep has a role to play in activating MMP3. However, Anpep as an exopeptidase typically cleaves neutral N-terminal amino acids from target proteins, whereas activation of MMP3 is more likely mediated by an endo-peptidase-like agent (Page-McCaw et al. 2007). However as the in vivo activator of MMP3 is yet to be unequivocally defined [although plasmin has been suggested as a potential activator (Fu et al. 2001)] it is possible that Anpep might activate MMP3 via an indirect mechanism.

Anpep deficiency (as deficiency for MMP3 or MMP2) does not significantly impair lactation. These results are also consistent with our finding that at day 18 of gestation and during lactation no significant differences between whole mounts of wild-type and Anpep deficient mice can be detected (data not shown). At these stages the whole mammary tissue is filled with epithelial cells. Expression of the Anpep gene is sustained slightly longer than that of MMP3, as has been demonstrated in three different micro-array analyses of mouse mammary development (Master et al. 2002; Stein et al. 2004; Clarkson et al. 2004). However the relative contribution of Anpep to duct formation amongst a significant number of other proteolytic enzymes may be more critical at earlier stages of gestation (Sorrell et al. 2005). Overall this suggests that Anpep deficiency delays rather than impairs mammary development.

Anpep plays an important role in angiogenesis (Rangel et al. 2007b). In that context Anpep was shown to be essential for the invasion of endothelium into stromal tissue or an implanted extra-cellular matrix plug. There are similarities between angiogenesis and mammary morphogenesis (Friedl and Gilmour 2009). However, whether the deficiency of angiogenesis and mammary branching morphogenesis in Anpep deficient mice derive from the same molecular events is unclear. Intriguingly, angiogenesis in the mammary gland has also been shown to impact on gland development and lactational performance in

mice. This has been demonstrated using mice carrying a tissue-specific inactivation of the VEGF gene in the mammary gland (Rossiter et al. 2007). However the most significant role of VEGF appears to occur during late pregnancy and early lactation. In contrast the effect of Anpep deficiency is most pronounced in mid-lactation suggesting that the proteolytic activity of Anpep rather than its angiogenic role have a major impact on mammary morphogenesis. However, recent findings in tumor allograft models have demonstrated a role for Anpep in tumor tissue and surrounding stromal tissue (Guzman-Rojas et al. 2012), suggesting that Anpep may fulfil more than one function in tissue development.

Acknowledgments The work was supported by the EU framework VI project grant (QOL-2000-00874) and the Hannah Development Fund.

References

Alexander CM, Selvarajan S, Mudgett J, Werb Z (2001) Stromelysin-1 regulates adipogenesis during mammary gland involution. J Cell Biol 152(4):693–703

Atherton AJ, Monaghan P, Warburton MJ, Gusterson BA (1992) Immunocytochemical localization of the ectoenzyme aminopeptidase N in the human breast. J Histochem Cytochem 40(5):705–710

Atherton AJ, Anbazhagan R, Monaghan P, Bartek J, Gusterson BA (1994a) Immunolocalisation of cell surface peptidases in the developing human breast. Differentiation 56(1–2): 101–106

Atherton AJ, O'Hare MJ, Buluwela L, Titley J, Monaghan P, Paterson HF, Warburton MJ, Gusterson BA (1994b) Ectoenzyme regulation by phenotypically distinct fibroblast sub-populations isolated from the human mammary gland. J Cell Sci 107(Pt 10):2931–2939

Benaud C, Dickson RB, Thompson EW (1998) Roles of the matrix metalloproteinases in mammary gland development and cancer. Breast Cancer Res Treat 50(2):97–116

Bhagwat SV, Lahdenranta J, Giordano R, Arap W, Pasqualini R, Shapiro LH (2001) CD13/APN is activated by angiogenic signals and is essential for capillary tube formation. Blood 97(3):652–659

Clarkson RW, Wayland MT, Lee J, Freeman T, Watson CJ (2004) Gene expression profiling of mammary gland development reveals putative roles for death receptors and immune mediators in post-lactational regression. Breast Cancer Res 6(2):R92–R109

Crawford HC, Matrisian LM (1996) Mechanisms controlling the transcription of matrix metalloproteinase genes in normal and neoplastic cells. Enzyme Protein 49(1–3): 20–37

Delmas B, Gelfi J, Kut E, Sjostrom H, Noren O, Laude H (1994) Determinants essential for the transmissible gastroenteritis virus-receptor interaction reside within a domain of aminopeptidase-N that is distinct from the enzymatic site. J Virol 68(8):5216–5224

Farrelly N, Lee YJ, Oliver J, Dive C, Streuli CH (1999) Extracellular matrix regulates apoptosis in mammary epithelium through a control on insulin signaling. J Cell Biol 144(6): 1337–1348

Friedl P, Gilmour D (2009) Collective cell migration in morphogenesis, regeneration and cancer. Nat Rev Mol Cell Biol 10(7):445

Fu X, Kassim SY, Parks WC, Heinecke JW (2001) Hypochlorous acid oxygenates the cysteine switch domain of pro-matrilysin (MMP-7). A mechanism for matrix metalloproteinase activation and atherosclerotic plaque rupture by myeloperoxidase. J Biol Chem 276(44):41279–41287

Gilmore AP, Metcalfe AD, Romer LH, Streuli CH (2000) Integrin-mediated survival signals regulate the apoptotic function of Bax through its conformation and subcellular localization. J Cell Biol 149(2):431–446

Guzman-Rojas L, Rangel R, Salameh A, Edwards JK, Dondossola E, Kim Y-G, Saghatelian A, Giordano RJ, Kolonin MG, Staquicini FI, Koivunen E, Sidman RL, Arap W, Pasqualini R (2012) Cooperative effects of aminopeptidase N (CD13) expressed by nonmalignant and cancer cells within the tumor microenvironment. Proc Nat Acad Sci 109(5):1637–1642. doi:10.1073/pnas.1120790109

Jerry DJ, Kuperwasser C, Downing SR, Pinkas J, He C, Dickinson E, Marconi S, Naber SP (1998) Delayed involution of the mammary epithelium in BALB/c-p53null mice. Oncogene 17(18):2305–2312

Kolb AF, Siddell SG (1997) Genomic targeting of a bicistronic DNA fragment by Cre-mediated site-specific recombination. Gene 203(2):209–216

Lassnig C, Sanchez CM, Egerbacher M, Walter I, Majer S, Kolbe T, Pallares P, Enjuanes L, Muller M (2005) Development of a transgenic mouse model susceptible to human coronavirus 229E. Proc Natl Acad Sci U S A 102(23): 8275–8280

Li M, Hu J, Heermeier K, Hennighausen L, Furth PA (1996) Apoptosis and remodeling of mammary gland tissue during involution proceeds through p53-independent pathways. Cell Growth Differ 7(1):13–20

Lilla J, Stickens D, Werb Z (2002) Metalloproteases and adipogenesis: a weighty subject. Am J Pathol 160(5):1551–1554

Lund LR, Romer J, Thomasset N, Solberg H, Pyke C, Bissell MJ, Dano K, Werb Z (1996) Two distinct phases of apoptosis in mammary gland involution: proteinase-independent and -dependent pathways. Development 122(1): 181–193

Lund LR, Romer J, Bugge TH, Nielsen BS, Frandsen TL, Degen JL, Stephens RW, Dano K (1999) Functional overlap between two classes of matrix-degrading proteases in wound healing. EMBO J 18(17):4645–4656

Master SR, Hartman JL, D'Cruz CM, Moody SE, Keiper EA, Ha SI, Cox JD, Belka GK, Chodosh LA (2002) Functional microarray analysis of mammary organogenesis reveals a developmental role in adaptive thermogenesis. Mol Endocrinol 16(6):1185–1203

Page-McCaw A, Ewald AJ, Werb Z (2007) Matrix metalloproteinases and the regulation of tissue remodelling. Nat Rev Mol Cell Biol 8(3):221–233

Rangel R, Sun Y, Guzman-Rojas L, Ozawa MG, Sun J, Giordano RJ, Van Pelt CS, Tinkey PT, Behringer RR, Sidman RL, Arap W, Pasqualini R (2007a) Impaired angiogenesis in aminopeptidase N-null mice. PNAS 104(11):4588–4593. doi:10.1073/pnas.0611653104

Rangel R, Sun Y, Guzman-Rojas L, Ozawa MG, Sun J, Giordano RJ, Van Pelt CS, Tinkey PT, Behringer RR, Sidman RL, Arap W, Pasqualini R (2007b) Impaired angiogenesis in aminopeptidase N-null mice. Proc Natl Acad Sci U S A 104(11):4588–4593

Rossiter H, Barresi C, Ghannadan M, Gruber F, Mildner M, Fadinger D, Tschachler E (2007) Inactivation of VEGF in mammary gland epithelium severely compromises mammary gland development and function. FASEB J 21(14):3994–4004. doi:10.1096/fj.07-8720com

Schedin P, Strange R, Mitrenga T, Wolfe P, Kaeck M (2000) Fibronectin fragments induce MMP activity in mouse mammary epithelial cells: evidence for a role in mammary tissue remodeling. J Cell Sci 113(Pt 5):795–806

Sorrell DA, Szymanowska M, Boutinaud M, Robinson C, Clarkson RW, Stein T, Flint DJ, Kolb AF (2005) Regulation of genes encoding proteolytic enzymes during mammary gland development. J Dairy Res 72(4):433–441

Stein T, Morris JS, Davies CR, Weber-Hall SJ, Duffy MA, Heath VJ, Bell AK, Ferrier RK, Sandilands GP, Gusterson BA (2004) Involution of the mouse mammary gland is associated with an immune cascade and an acute-phase response, involving LBP, CD14 and STAT3. Breast Cancer Res 6(2):R75–R91

Sternlicht MD, Lochter A, Sympson CJ, Huey B, Rougier JP, Gray JW, Pinkel D, Bissell MJ, Werb Z (1999) The stromal proteinase MMP3/stromelysin-1 promotes mammary carcinogenesis. Cell 98(2):137–146

Tonner E, Barber MC, Allan GJ, Beattie J, Webster J, Whitelaw CBA, Flint DJ (2002) Insulin-like growth factor binding protein-5 (IGFBP-5) induces premature cell death in the mammary glands of transgenic mice. Development 129(19):4547–4557

Winnicka B, O'Conor C, Schacke W, Vernier K, Grant CL, Fenteany FH, Pereira FE, Liang B, Kaur A, Zhao R, Montrose DC, Rosenberg DW, Aguila HL, Shapiro LH (2010) CD13 is dispensable for normal hematopoiesis and myeloid cell functions in the mouse. J Leukoc Biol 88(2):347–359. doi:10.1189/jlb.0210065

Wiseman BS, Sternlicht MD, Lund LR, Alexander CM, Mott J, Bissell MJ, Soloway P, Itohara S, Werb Z (2003) Site-specific inductive and inhibitory activities of MMP-2 and MMP-3 orchestrate mammary gland branching morphogenesis. J Cell Biol 162(6):1123–1133

Witty JP, Wright JH, Matrisian LM (1995) Matrix metalloproteinases are expressed during ductal and alveolar mammary morphogenesis, and misregulation of stromelysin-1 in transgenic mice induces unscheduled alveolar development. Mol Biol Cell 6(10):1287–1303

Yeager CL, Ashmun RA, Williams RK, Cardellichio CB, Shapiro LH, Look AT, Holmes KV (1992) Human aminopeptidase N is a receptor for human coronavirus 229E. Nature 357(6377):420–422